Generation of Glass Structures for Molecular Simulations of Polymers Containing Large Monomer Units: Application to Polystyrene

Rajesh Khare and Michael E. Paulaitis*

Center for Molecular and Engineering Thermodynamics, Department of Chemical Engineering, University of Delaware, Newark, Delaware 19716

Steven R. Lustig

Central Research, The DuPont Company, Experimental Station, Wilmington, Delaware 19880-0356

*Received June 18, 1993; Revised Manuscript Received October 1, 1993**

ABSTRACT: We describe a method for generating glass structures of polymers containing large monomer units for use in molecular simulations. This method is an extension of the technique proposed by Rigby and Roe (Rigby, D.; Roe, R. *J. Chem. Phys.* **1987**, *87*, 7285) for short-chain alkanes and involves a "polymerization" of randomly placed monomers in the simulation box. An optimum polymerization sequence is found by the technique of simulated annealing, and a well relaxed glass structure is generated from this sequence by a combination of molecular mechanics and molecular dynamics simulations. We have used the technique to prepare 10 glass structure of polystyrene, for which we have calculated average structural properties. The amorphous nature of these structures is demonstrated by the absence of long-range orientational correlations for the chain backbone. The phenyl rings also show a preference to pack at a distance of 5–6 Å and to align at right angles to one another.

Introduction

Many macroscopic mechanical and transport properties of amorphous polymers are intimately related to their chemical structure through the effects of chain packing and localized chain motions. In recent years, molecular simulations have emerged as a valuable tool for understanding these relationships and the various theories and mechanisms that govern both static and dynamic properties of polymers. Applications include investigations of the structure of glasses,[1] the glass transition,[2] polymer–wall interactions,[3] sorption of small molecules in polymers,[4–7] adsorption of polymers on solid surfaces,[8] and thermal degradation of polymers.[9]

For molecular simulations of polymer glasses, an important consideration is the generation of well-relaxed glass structures at realistic densities. However, the connectivity of the polymer chain makes this problem more difficult than, for example, generating glass structures of small molecules. The usual procedure for preparing a polymer glass consists of two steps: obtaining a reasonable initial structure and then processing this structure to obtain a well-relaxed glass.[1,10] For polymers containing large monomer units, these methods can encounter difficulties that require additional preparatory stages in both steps.[11] When relatively large systems are needed—for example, in simulations of diffusion in polymers[12]—these additional stages can place severe demands on the computational efficiency of the glass-generating procedure. In this work, we propose a method for obtaining well-relaxed glass structures of such polymers and apply this method to polystyrene.

Previous Work

A polymer glass can be generated from either an equilibrium liquid structure[2,13–15] or a reasonable initial guess for the glass structure.[1,11,16,17] Boyd and co-workers obtained glass structures for polyethylene by starting with an equilibrium liquid.[13–15] In their approach, an ordered array of planar all-trans chains was melted down by Monte Carlo simulation in a periodic box to form the equilibrium liquid, which was then energy minimized to obtain the glass. The system volume was treated as a degree of freedom in the minimization to simulate the densification that takes place when the glass is quenched from the equilibrium melt.

Rigby and Roe[2] used a different approach to produce initial liquid structures in their method for generating glasses of short-chain alkanes consisting of 10, 20, or 50 monomer units. First, a random spatial distribution of methylene groups was prepared, and groups in close proximity were joined to form several polymer chains. This system was then equilibrated by molecular dynamics simulation using reduced force constants for all interactions except the nonbonded interactions. The force constants were gradually increased to their desired values as the bond lengths and angles relaxed to their equilibrium values. Glasses were obtained from this liquid by molecular dynamics simulation with stepwise cooling.

Another method for generating polymer chains in either the melt or the glass state is to grow the chains in a sequential bond-by-bond fashion. McKechnie et al.[10] noted difficulties with this method due to excluded-volume effects when generating structures for polyethylene and, hence, modified the technique to permit steric overlaps of the chain segments. These overlaps were then eliminated by molecular dynamics simulation with a modified Lennard-Jones potential in which repulsive nonbonded interactions between segments at short distances were attenuated by assuming a constant, finite force. A similar approach has also been proposed for generating structures of short-chain liquid alkanes at high densities in which chain growth and equilibration of the liquid structure proceed simultaneously in a Monte Carlo simulation.[18]

In principle, the methods for generating liquid structures can be used to prepare glass structures directly. However, since the glass will have a higher density than the polymer

* Abstract published in *Advance ACS Abstracts*, November 15, 1993.

0024-9297/93/2226-7203$04.00/0

liquid, the problem of steric overlap becomes even more formidable, and hence it is more difficult to generate glass structures at realistic densities. The direct generation of a polymer glass was first carried out by Theodorou and Suter[1] in their pioneering study of polypropylene glass. In this approach, an initial guess for the glass structure was obtained by Monte Carlo chain growth in a periodic box using probabilities for bond angles given by the rotational isomeric state (RIS) model.[19] These initial structures were found to have a high potential energy and a nonuniform spatial distribution. As a consequence, the Monte Carlo algorithm was modified by adjusting the RIS probabilities to account for nonbonded interactions between carbons along the chain that are separated by five or more bonds. The initial structures obtained by this procedure were then relaxed to mechanical equilibrium by stagewise energy minimization. The technique has also been applied to polycarbonate,[11] polysulfone,[16] and poly(vinyl chloride).[17]

The efficiency of all these methods will suffer, to some extent, when applied to polymers with large monomer units. For example, when the method of Theodorou and Suter was applied to polycarbonate,[11] energy minimization of the initial glass structures required more than 25 processing stages (compared to 3 stages for polypropylene) in which the van der Waals radii and partial charges were increased gradually to their desired values. The difficulty encountered in these energy minimizations can be attributed to the added complexity of electrostatic interactions and, more importantly, to the bulkiness of the large monomer unit. The latter can give rise to severe steric overlaps in initial structures that, in turn, are difficult to energy minimize. The problem of steric overlaps in initial glass structures is avoided completely in the method proposed by Gupta et al.[18] In this method, chain growth and equilibration proceed in tandem, such that chain growth occurs only if a monomer can be added without steric overlap. However, the method is not expected to be computationally efficient for polymers containing large monomer units, since longer equilibration times will be needed to form a sufficiently large cavity near the end of the chain for chain growth to take place. We propose an alternative method in this work in which one starts with a configuration of the desired number of monomers in a simulation box. These monomers are then connected in an optimal polymerization sequence by applying the technique of simulated annealing,[20] and bond lengths and angles are subsequently relaxed to generate a polymer glass structure. Since no new monomers are added to the box during this procedure, the problems of steric overlaps and spatially nonuniform distributions of chain segments are not encountered. The computational burden is therefore shifted from one of alleviating severe steric overlaps to that of finding the optimal connectivity of the monomers.

Glass Generation Method

Our approach for generating glass structures is implemented in the following three stages: (1) generate a configuration of monomers placed randomly in the simulation box; (2) connect monomer units in an optimal polymerization sequence; and (3) minimize the energy of this structure to obtain a well-relaxed polymer glass.

In the first stage, the monomers are initially placed in the simulation box in an ordered array. The number of monomers is predetermined by the temperature and pressure of interest to give the experimental density of the polymer. The system is then heated and relaxed by molecular dynamics at an elevated temperature. It should be emphasized that our purpose at this stage of the procedure is to achieve a uniform spatial distribution and a random orientational distribution of monomers in the simulation box, and not an equilibrium liquid. We have found that, in general, 5–10 ps of molecular dynamics simulation is sufficient to obtain such distributions. A random distribution of orientations is facilitated by reducing all atomic radii in this stage.

A "polymerization" of this configuration is then carried out in the second stage by connecting spatially adjacent monomers. Periodic boundary conditions are employed to eliminate surface effects, and the minimum image convention is used; i.e., the distance between any two monomers is considered to be the distance between the nearest periodic images of the monomers. The problem of connecting a given number of monomers to form the shortest polymer chain is similar to the classical "Traveling Salesman" problem[20] with one obvious exception: The two ends of the polymer chain are not connected to form a closed circuit. In principle, the technique could also be modified to connect the chain ends and thereby avoid the strong free-volume bias that can occur near them. The Traveling Salesman problem has been solved previously by simulated annealing,[20] a multivariable optimization technique based on the Monte Carlo method. The algorithm as described by Press et al.[21] is used here with only minor modifications: After connecting monomers in an initial polymerization sequence, simulated annealing is carried out by randomly altering this sequence and evaluating the cost of each move in terms of its effect on the total chain length of the polymer. Moves are either accepted or rejected on the basis of standard Metropolis probabilities.

Many of the bond lengths and bond angles in the polymer chain backbone at the end of this stage will have values far from their equilibrium values, and hence the potential energy of this structure must be minimized primarily with respect to these degrees of freedom. This is carried out in the third stage of our method. Since there will be multiple local minima on the potential energy surface, we minimize the energy so that the structure reaches one of these local minima. In this work, the structures are relaxed using a combination of energy minimization and molecular dynamics at elevated temperature.

Application to Polystyrene

A detailed, atomistic model of polystyrene is used in which all atoms are treated explicitly and electrostatic interactions are accounted for by placing partial charges on the atoms. The computational effort could be reduced considerably by applying the united atom approximation and collapsing the hydrogen atoms into their respective carbon atoms. However, a future objective of this work is to study phenyl ring rotation in the glass, and calculations on single chains of this polymer have shown that cooperative motion of the phenyl ring and the backbone is affected by interactions between the ortho hydrogens on the ring and the hydrogens attached to backbone carbons.[22–25] Furthermore, electrostatic interactions between the phenyl rings will influence both the local packing of these rings[26–30] and the backbone conformations of polystyrene.[29] Thus, we have chosen to treat all hydrogen atoms explicitly.

The CHARMM force field expressions and parameters were used to model bond stretching, bond angle bending, torsional angle rotation, and the van der Waals contribution to nonbonded interactions.[31] Equilibrium values of the bond lengths and bond angles were set equal to the

Table I. Partial Charges on Various Atomic Species

atom type	charge[a]	atom type	charge[a]
$C(CH_2)$	−0.15	C_{phenyl}[b]	−0.065
$H(CH_2)$	0.095	C_{phenyl}	−0.13
C(CHR)	−0.07	H_{phenyl}	0.13
H(CHR)	0.095		

[a] Elementary Charge Units. [b] Phenyl carbon bonded with C(CHR).

values used by Yoon et al.[32] Electrostatic interactions were described by the CHARMM force field expression, but with a distance-dependent dielectric constant based on the Block and Walker approximation[11,17] and partial charges determined by a Mulliken population analysis of AM1 semiempirical molecular orbital calculations on polystyrene dimers and trimers. The calculated values of these partial charges are given in Table I. The dielectric constant has the following functional form:

$$D(r) = 1 \qquad r < a$$

$$D(r) = \epsilon_B \exp(-\kappa/r) \qquad r \geq a$$

$$\kappa = a \ln \epsilon_B$$

where the bulk dielectric constant, ϵ_B, is set equal to 2.55[33] and a is 2.9 Å for all atom pairs. All nonbonded interactions are truncated at a distance of 9.0 Å.

One particular parameter that required special consideration for polystyrene was the energy barrier for intrinsic torsional rotation of the phenyl ring. Calculations of the energy barrier for cooperative ring rotation in single chains of polystyrene[25] and in the protein tosyl α-chymotrypsin,[34] carried out with and without this intrinsic torsional barrier, have shown that the energy barrier is approximately the same in either case. These observations suggest that the barrier for ring rotation is determined primarily by the nonbonded interactions between the phenyl ring atoms and neighboring atoms, rather than the barrier for intrinsic torsional rotation. Hence, all the calculations reported here have been carried out without an intrinsic torsional barrier for phenyl ring rotation. Our in-house modification of the CHARMM source code was used for all calculations.

Bulk polystyrene glasses consisting of a parent chain (degree of polymerization = 40) and its images were generated in a cubic box with an edge length of 18.75 Å. This box size gives a polymer density of 1.05 g/mL, which corresponds to the experimental value for atactic polystyrene at room temperature.[33] The starting configuration of 40 monomers was heated to 600 K and maintained at this temperature for approximately 5–10 ps. During this process, the atomic radii were set to 75% of their desired values. This procedure provides one starting configuration for subsequent processing. Other starting configurations were generated from this one by running molecular dynamics and selecting configurations at intervals of 5–10 ps.

An optimal polymerization sequence was then obtained for each configuration, as described above. A configuration was accepted for further processing only if the polymer chain had a reasonable end-to-end distance compared to experimental values. This initial screening process was based on the observation that, during the subsequent energy minimization, the end-to-end distance did not change significantly; i.e., the connected monomer units would reorient about their positions, rather than translate, to give the correct bond lengths and bond angles. If a configuration did not yield a satisfactory end-to-end distance, it was rejected and another optimal polymerization sequence was obtained by simulated annealing. We found that, in general, no more than three attempts were required to obtain a chain configuration with a satisfactory end-to-end distance. The computational cost associated with repeating the simulated annealing step in this screening process was negligible compared to other computational costs, most notably, in the energy minimizations.

The chain configuration thus obtained was minimized with respect to the potential energy in two steps. In the first, no partial charges were used and all atomic radii remained at 75% of their desired values. In the second step, the chains were minimized again with the desired values for atomic radii and partial charges. Typically only 300–400 steps of the Powel minimization method were required in each of these steps. Although not essential, we chose not to minimize the structures completely in the two steps, but ran molecular dynamics for 5 ps at 300–400 K and then minimized a second time until the gradient of the energy vanished.

A minor complication arises when applying this method to vinyl polymers. A random distribution of diads will be obtained in which the fraction of meso diads is approximately 0.5. However, in atactic polystyrene, the meso and racemic diads obey Bernoullian statistics, but the fraction of meso diads is found to be between 0.3 and 0.5.[32,35,36] Therefore, meso diads in *mm* sequences of the chain were chosen randomly and the chirality of asymmetric carbon was changed in the first minimization step. This procedure was repeated until the fraction of meso diads reached a value of ~0.35.

Results

The properties reported in this work represent average values for an ensemble of 10 glass structures. Nine of these structures have end-to-end distances in the range 39–57 Å, while the remaining structure has an end-to-end distance of 67 Å. For comparison, the calculated root-mean-square end-to-end distance for a polystyrene 40-mer based on measurements of intrinsic viscosity is 47.5 Å.[37] Since the polymer chains were screened to give end-to-end distances in reasonable agreement with this value, this property is essentially a fitted property of our structures. It should be noted that no correlations were observed between this chain dimension and the properties calculated below.

Cohesive Energy Density and Solubility Parameter. The cohesive energy, U_{coh}, is defined as the intermolecular or interchain contribution to the total potential energy of the system.[1] Thus,

$$U_{coh} = U_{pc} - U_{tot} \qquad (1)$$

where U_{tot} is the potential energy of a glass structure in our periodic box and U_{pc} is the energy of an isolated parent chain that consists of only intramolecular contributions (i.e., an isolated chain in the absence of periodic boundary conditions). We obtained U_{coh} = 138(±8) kcal/mol for our 10 glass structures, which corresponds to a value for Hildebrand's solubility parameter of $\delta = 12.06 \times 10^3$ (J/m^3)$^{1/2}$. This value of the solubility parameter is ~65% of the experimentally derived value reported for polystyrene.[33] However, it should be noted that the cohesive energy was calculated without a correction to account for truncating the nonbonded interactions in the potential function at finite distances, and it was found in previous work[1,17] that such tail corrections can be significant. Although better agreement with experiment could be obtained if we applied this correction, the actual value of the correction for the electrostatic interactions would be obtained by finding a small difference between large

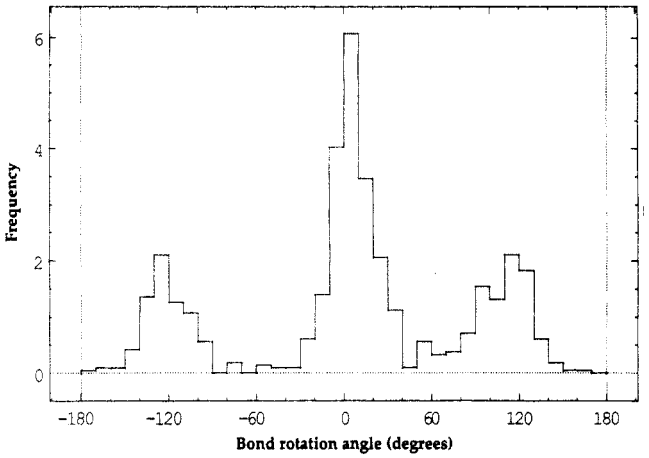

Figure 1. Distribution of torsional angles for backbone bonds averaged over the 10 glass structures.

Table II. Probabilities of Rotational Isomeric States for Backbone Torsional Angles

rotational isomeric state	angle (ϕ_i) interval (deg)	a priori probability from RIS model: of Yoon et al.[32]	a priori probability from RIS model: of Rapold and Suter[29]	probability from the model structures
t	$-60 \le \phi_i \le 60$	0.732	0.756	0.548
g^+	$60 < \phi_i \le 180$	0.268	0.244	0.252
g^-	$-180 \le \phi_i < -60$			0.200

numbers and thus would not be highly reliable. Since the structure of bulk polymer glasses will be determined primarily by short-range repulsive interactions in the potential function,[38,39] the long-range attractive interactions represented by this correction can be neglected when structural properties on the length scale of the simulation box are considered.

Chain Conformation in the Bulk. Since no information regarding the conformational properties of the polymer is incorporated directly into our procedure, important properties to consider in evaluating the glass structures that have been generated are those characterizing the conformations of polymer chains. These conformations are described by the torsional angles for the backbone bonds and the orientation of the phenyl rings with respect to the chain backbone. The distribution of backbone torsional angles for our 10 structures is shown in Figure 1, where the torsional angles are assigned values according to the convention introduced by Flory et al.[40] As expected, this distribution is peaked about the rotational isomeric t and g^+ states, which appear to overlap slightly, and also about the g^- state. The fraction of torsional angles in the t state is 0.55, which is significantly higher than that corresponding to a random distribution of torsional angles (i.e., 0.33). We believe that the nonrandom distribution can be attributed to space-filling requirements[18] and our screening process of choosing only those chain conformations with reasonable end-to-end distances. The average a priori probabilities of the rotational isomeric states for the backbone torsional angles in polystyrene were also calculated from the RIS model by use of matrix multiplication techniques.[19] This calculation was done by generating 100 Bernoullian configurations with a degree of polymerization of 100 and an expected fraction of meso diads of 0.35. These values calculated using the RIS model proposed by Yoon et al.,[32] and the model proposed by Rapold and Suter,[29] are compared in Table II with those obtained from our structures. Our ensemble of glass structures has a lower population of backbone torsional angles in the t state and a higher population in the g^- state compared to RIS model predictions. Similar results were observed in earlier studies on polypropylene[1] and poly(vinyl chloride)[17] and were attributed to the glass generation method used in those studies. This method was entirely different from the one described here.

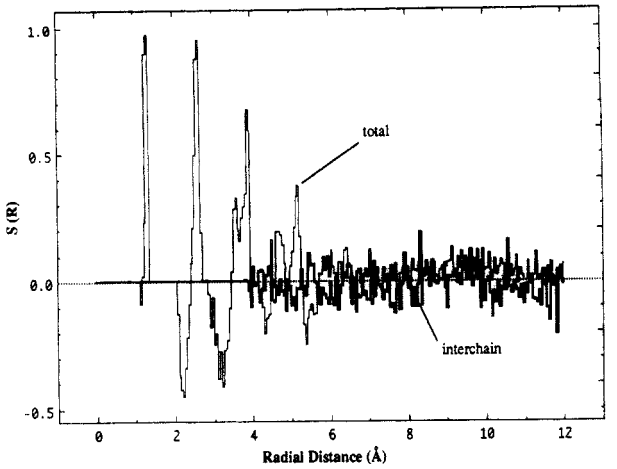

Figure 2. Total (thin line) and interchain (thick line) orientation correlation functions for the backbone bonds.

Glass Structure. The local orientation of the backbone can be characterized by the bond orientational correlation function defined by

$$S(R) = \frac{1}{2}[3\langle \cos^2 \theta \rangle - 1]$$

where θ is the angle between any two bond chords along the chain backbone, and $\langle ... \rangle$ denotes the average over all pairs of bond chords separated by a distance R. Bond chord i is defined as the chord joining the midpoints of the backbone bonds flanking carbon i. Positive values of $S(R)$ indicate a tendency for parallel alignment, while negative values indicate a preference for alignment at right angles. Figure 2 shows a plot of $S(R)$ as a function of R. The contribution due exclusively to interchain correlations, defined by considering only those pairs of bond chords belonging to different images of the parent chain, oscillates about zero for all separations greater than 4 Å, indicating that there is no interchain orientational order in our structures. The total correlation function, containing both intrachain and interchain contributions, shows a strong tendency for parallel alignment at distances less than 6 Å due to near-neighbor intrachain correlations. At larger separations, the total correlation function oscillates about zero, indicating that there is also no intrachain orientational order in our structures. Thus, these structures can be considered amorphous over the length scale of the simulation.

A similar orientational correlation function can be defined to characterize orientational correlations between phenyl rings. In this case, the angle θ is the angle between vectors normal to the planes of two phenyl rings separated by a distance R. The order parameter $S(R)$ for ring–ring orientational correlations is shown in Figure 3. The peak in the total correlation function at 4 Å is due exclusively to intrachain contributions from the nearly parallel alignment of nearest-neighbor phenyl rings. Two factors contribute to this alignment: first, the rings are forced to lie at right angles to the backbone because of steric repulsions between the rings and the backbone, and second, the backbone bonds themselves exhibit a strong tendency for parallel alignment at short separations, as was shown in Figure 2. The interchain correlation function is zero for separations less than 4 Å, but indicates a tendency for

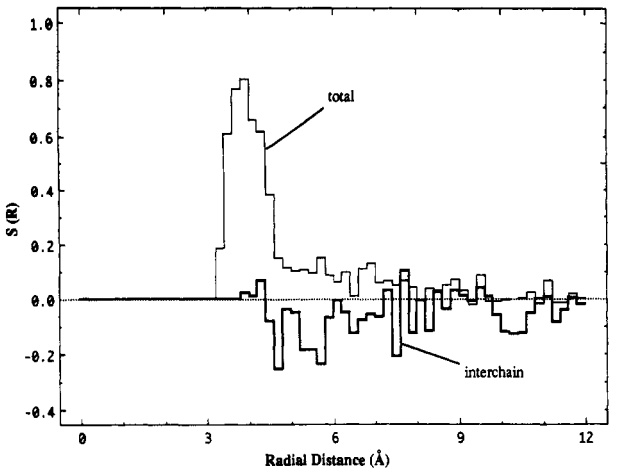

Figure 3. Total (thin line) and interchain (thick line) orientation correlation functions for phenyl rings. Radial distance is defined as the distance between ring centroids.

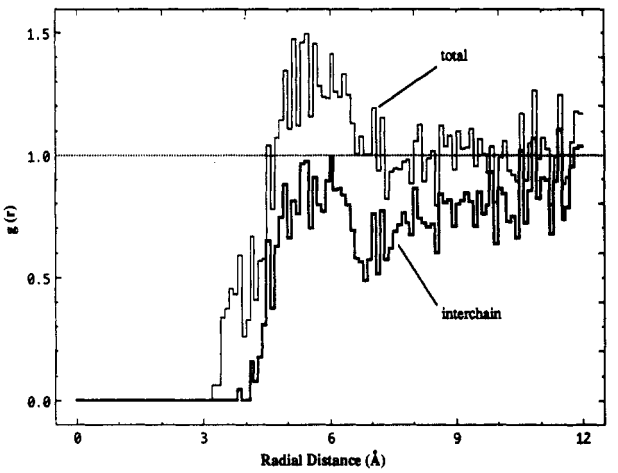

Figure 4. Total (thin line) and interchain (thick line) radial distribution functions for phenyl rings. Radial distance is defined as the distance between ring centroids.

alignment at right angles at separations of 4–6 Å. Similar observations have been made for the packing of aromatic side chains in protein crystals and have been attributed to weak interactions between the aromatic rings resulting from their quadrupole moments.[30] For larger separations, the orientational correlations are lost and the total correlation approaches zero.

The glass structure can also be characterized by pair correlation or radial distribution functions (RDFs) for the different atoms. The pair correlation function $g_{AB}(r)$ for atoms A and B represents the probability of finding these two atoms separated by a distance r relative to the probability of finding them at the same separation in the absence of any A–B correlations. The ring–ring RDF is shown in Figure 4. At distances between 3 and 4 Å, the total correlation function has only intrachain contributions arising from nearest-neighbor ring contacts. However, both the total and interchain correlation functions show a broad peak at ~5.5 Å, indicating preferential packing of the phenyl rings in the amorphous glass at this separation. It is interesting to note that a peak near 5.5 Å is also observed in a related pair correlation function for aromatic side chains in protein crystals.[30] There also appears to be a second peak in the total correlation function at a separation of ~9 Å, which presumably corresponds to the second nearest-neighbor shell and suggests an oscillatory behavior for the radial distribution function.

Figure 5 shows the total and interchain RDFs for the phenyl ring carbon atoms (i.e., for C_{phenyl}–C_{phenyl} pairs as

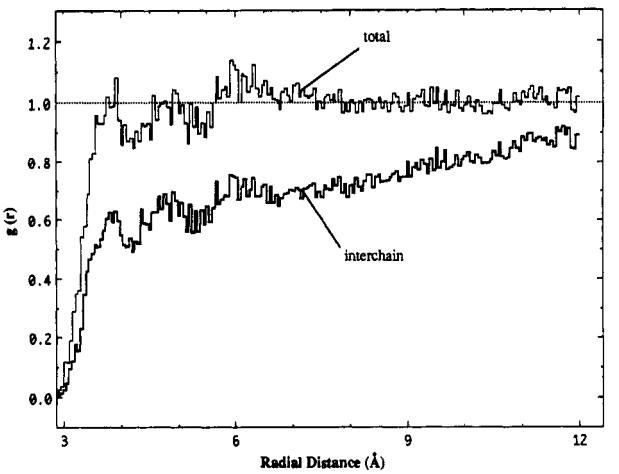

Figure 5. Total (thin line) and interchain (thick line) radial distribution functions for C_{phenyl}–C_{phenyl} pairs.

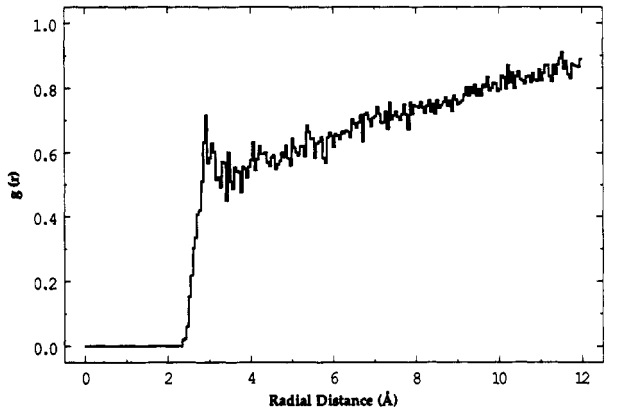

Figure 6. Interchain radial distribution function for C_{phenyl}–H_{phenyl} pairs.

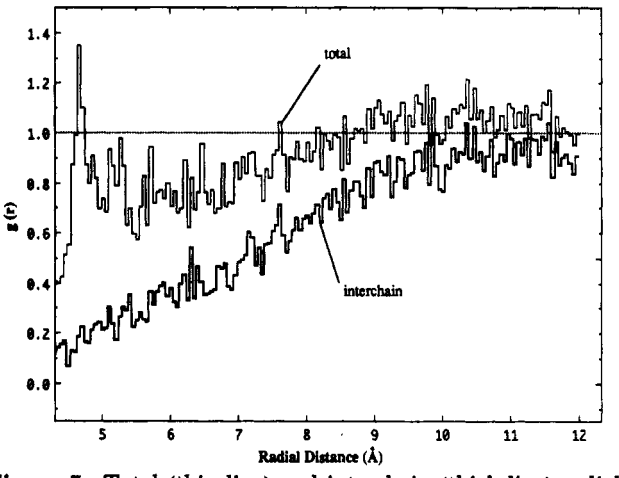

Figure 7. Total (thin line) and interchain (thick line) radial distribution functions for $C_{backbone}$–$C_{backbone}$ pairs.

defined in Table I). Both RDFs have peaks at 4, 5, and 6 Å. Figure 6 shows the interchain RDF for C_{phenyl}–H_{phenyl} pairs, which exhibits a sharp peak at ~3 Å. Both of these results are consistent with our earlier observations that the phenyl rings on different chains pack preferentially at a separation of ~6 Å and have a tendency to align at right angles to one another.

The RDF for the backbone carbons is shown in Figure 7. The total correlation function exhibits a number of sharp peaks at separations less than 5 Å that are not shown in the figure and reflect the connectivity of the backbone carbon atoms. However, the total correlation function is much less than unity over the range of separations from 5 to 8 Å. The lower probabilities at these distances can be

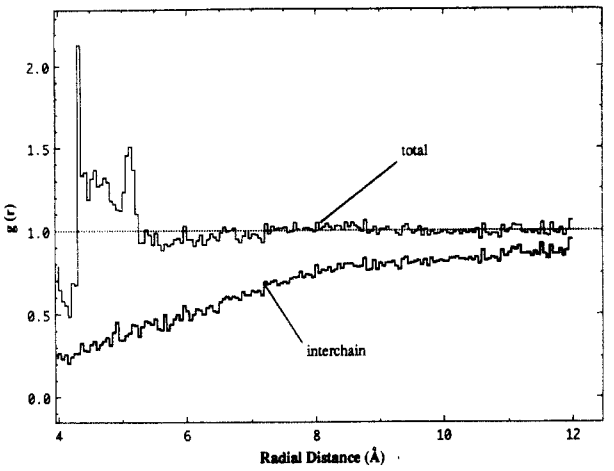

Figure 8. Total (thin line) and interchain (thick line) radial distribution functions for C_{phenyl}–$C_{backbone}$ pairs.

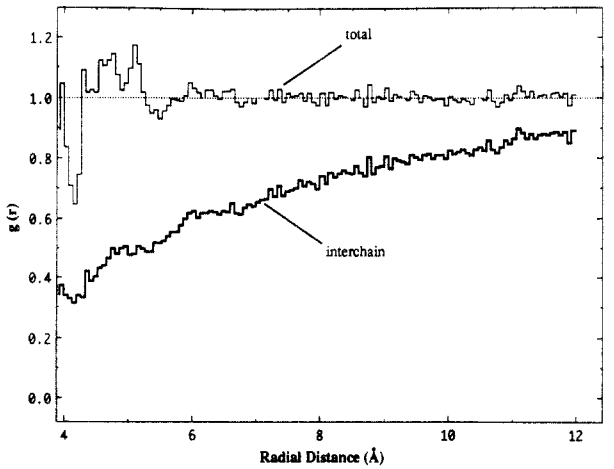

Figure 9. Total (thin line) and interchain (thick line) radial distribution functions for all carbon atoms.

attributed to the bulky phenyl rings which, on average, keep the backbone carbons separated by distances greater than 5–8 Å. The interchain carbon–carbon correlations increase more or less monotonically with increasing separation and approach unity at large separations, as does the total correlation function.

Figure 8 shows the RDF for C_{phenyl}–$C_{backbone}$ pairs. Intrachain contributions from carbons in the meta and para positions give the broad peak in the total correlation function over the range 4.3–5.2 Å. The total correlation function is essentially unity for separations greater than 7 Å, while the interchain contribution increases monotonically and approaches unity at much larger separations. The RDF for all carbon atoms in the polymer is shown in Figure 9. The interchain correlation function has broad humps at both 5 and 6 Å, while the total RDF shows a broad peak over the range 4.2–5.2 Å. Peaks in the RDF at 5 and 6 Å have also been observed in X-ray scattering experiments on atactic polystyrene glasses and have been attributed to various ring–ring and ring–backbone correlations.[41-43] Our results offer an interpretation of these observations recognizing that, to a reasonable approximation, the scattering experiments reflect primarily carbon–carbon pair correlations. That is, the observed peaks in the experimental RDF at 5 and 6 Å arise because of intrachain C_{phenyl}–$C_{backbone}$ pair correlations, as shown in Figure 8, and C_{phenyl}–C_{phenyl} pair correlations, as shown in Figure 5.

The radial distribution functions from our model structures can be used to predict the X-ray scattering structure factor for atactic polystyrene glass. In these

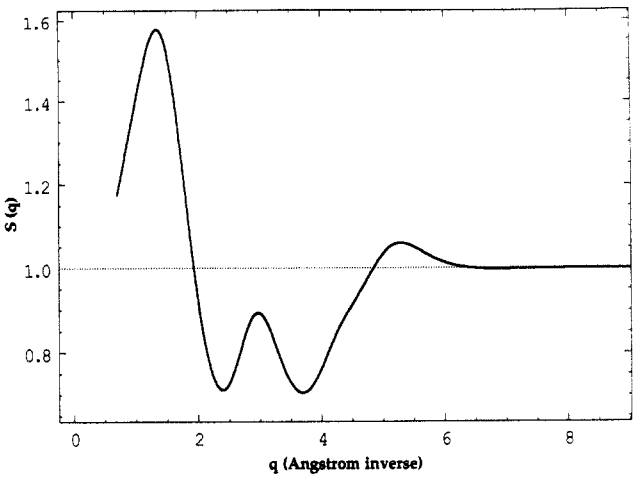

Figure 10. Calculated X-ray scattering structure factor as a function of the magnitude of the scattering vector $\mathbf{q} = (4\pi/\lambda) \sin\theta$.

calculations, we assume $g_{AB}(r) = 1$ for $r > 9.37$ Å (i.e., half the box length). The elastic structure factor, $S(\mathbf{q})$, was calculated using the method proposed by Theodorou[44] with atomic scattering factors obtained from literature.[45] A plot of $S(\mathbf{q})$ as a function of magnitude of the scattering vector, $\mathbf{q}$, is given in Figure 10. The calculated $S(\mathbf{q})$ shows a dominant peak at $\mathbf{q} = 1.3$ Å^{-1} and two additional peaks at $\mathbf{q} = 3.0$ and 5.3 Å^{-1}. These peak locations are in excellent agreement with those observed in X-ray scattering experiments on atactic polystyrene glass: a dominant peak at $\mathbf{q} = \sim 1.4$ Å^{-1} and two other peaks at 3.0 and 5.5 Å^{-1} in this range of $\mathbf{q}$ values.[42,46,47] A small peak is also observed in the scattering experiments at $\mathbf{q} = 0.75$ Å^{-1}.[42,46-48] However, we have truncated our radial distribution functions at $r = 9.37$ Å to avoid box size effect and, therefore, do not observe this peak in our results. Nevertheless, the results indicate that our model glass structures are credible representations of the actual glass structure of atactic polystyrene on the length scale of our simulations.

Conclusions

The method we have proposed has been applied to generating glass structures of polystyrene. These atomistic structures provide detailed information about both orientational and spatial correlations in the polymer glass. We have found no long-range orientational order for the chain backbones, indicating that these structures are amorphous on the length scale of the simulation box. The pair correlation functions for the phenyl rings show preferential packing at a distance of approximately 5–6 Å with a tendency to align at right angles to one another. Similar packing behavior has been reported in the literature for the aromatic side chains in protein crystals and has been attributed to enthalpically favorable quadrupolar interactions between the aromatic rings.

Generating the initial configuration of monomers by molecular dynamics simulation is a computational expense in this method that must be compared with, for example, the Monte Carlo generation of a polymer chain, as proposed by Theodorou and Suter.[1] The problems associated with severe steric overlaps that are encountered in Monte Carlo chain growth are not experienced in the approach taken here. Thus, the energy minimization of an initial polymer conformation to obtain a well-relaxed glass is potentially more efficient, although this advantage is expected to be modest in cases where the monomer unit is small in size. Special measures also have to be employed in Monte Carlo

chain growth to ensure that the resulting structures are spatially uniform. In the proposed method, the initial configuration of monomers is de facto uniformly distributed in the simulation box, and this spatial distribution does not change during the subsequent relaxation of the polymer structure. Hence, spatially uniform glass structures are assured.

Another issue is the somewhat lower fraction of backbone bonds in the trans state we obtained compared to that predicted by the RIS model. Similar results have also been reported for glasses of polypropylene[1] and poly(vinyl chloride)[17] generated by an entirely different method. In principle, the technique of heating structures to very high temperatures, followed by molecular dynamics at the desired temperature, can be used to relax the chain backbone to obtain the expected value for the fraction of trans states, as demonstrated by McKechnie et al.[10] However, even in the case of polyethylene, molecular dynamics simulations in excess of 200 ps were required to achieve the desired result because conformational relaxation at these temperatures is very slow.

A number of improvements can be considered in the implementation of this method, such as a rigid translation or rotation of the monomers in the "polymerization" step to obtain an initial polymer structure that would require less effort in the energy minimization step. Another improvement that could be implemented for polymers with relatively complicated monomer units—e.g., polycarbonate—would be to change the internal torsional angles within the monomer during the "polymerization". The method can also be extended to incorporate dissolved species within the polymer matrix for molecular simulations of polymer–diluent systems. Here, one can start with a configuration of the species of interest and monomers in the simulation box and then "polymerize" the monomers to obtain a polymer chain. The problems associated with solute insertion into a dense, amorphous polymer matrix can thus be avoided.

Both intrachain and interchain effects influence local conformational transitions and other chain motions in bulk polymers. Transition-state calculations of cooperative ring flip motions in single chains of polystyrene[25] are now being extended to the glass state using our model structures to investigate the effects of chain packing on this process.

Acknowledgment. We are grateful to C. L. Brooks, III, for providing us with the source code for the program CHARMM. We also thank U. W. Suter and R. Rapold for making available to us their unpublished results on the conformational characteristics of polystyrene. Financial support provided by the National Science Foundation (CPE 8351228) is also gratefully acknowledged.

References and Notes

(1) Theodorou, D. N.; Suter, U. W. *Macromolecules* **1985**, *18*, 1467.
(2) Rigby, D.; Roe, R. J. *J. Chem. Phys.* **1987**, *87*, 7285.
(3) Mansfield, K. F.; Theodorou, D. N. *Macromolecules* **1991**, *24*, 4295.
(4) Takeuchi, H.; Okazaki, K. *J. Chem. Phys.* **1990**, *92*, 5643.
(5) Takeuchi, H.; Roe, R. J.; Mark, J. E. *J. Chem. Phys.* **1990**, *93*, 9042.
(6) Muller-Plathe, F. *Macromolecules* **1991**, *24*, 6475.
(7) Sok, R. M.; Berendsen, J. C.; van Gunsteren, W. F. *J. Chem. Phys.* **1992**, *96*, 4699.
(8) Hentschke, R.; Schurmann, B. L.; Rabe J. P. *J. Chem. Phys.* **1992**, *96*, 6213.
(9) Nyden, M. R.; Forney, G. P.; Brown J. E. *Macromolecules* **1992**, *25*, 1658.
(10) McKechnie, J. I.; Brown, D.; Clark, J. H. R. *Macromolecules* **1992**, *25*, 1562.
(11) Hutnik, M.; Gentile, F. T.; Ludovice, P. J.; Suter, U. W.; Argon, A. S. *Macromolecules* **1991**, *24*, 5962.
(12) Bicerano, J. Dow Chemical Co., Midland, MI, personal communication, 1993.
(13) Boyd, R. H. *Macromolecules* **1989**, *22*, 2477.
(14) Boyd, R. H.; Pant, P. V. K. *Macromolecules* **1991**, *24*, 4073.
(15) Boyd, R. H.; Pant, P. V. K. *Macromolecules* **1991**, *24*, 4078.
(16) Fan, C. F.; Hsu, S. L. *Macromolecules* **1991**, *24*, 6244.
(17) Ludovice, P. J.; Suter, U. W. In *Computational Modeling of Polymers*; Bicerano, J., Ed.; Marcel Dekker: New York, 1992; p 401.
(18) Gupta, S.; Westermann-Clark, G. B.; Bitsanis, I. J. *Chem. Phys.* **1993**, *98*, 634.
(19) Flory, P. J. *Statistical Mechanics of Chain Molecules*; Wiley-Interscience: New York, 1969.
(20) Kirkpatrick, S.; Gelatt, C. D.; Vecchi, M. P. *Science* **1983**, *220*, 671.
(21) Press, W. H.; Teukolsky, S. A.; Vetterling, W. T.; Flannery, B. P. *Numerical Recipes in FORTRAN*; Cambridge University: Cambridge, U.K., 1992.
(22) Tonelli, A. E. *Macromolecules* **1973**, *6*, 682.
(23) Hagele, P. C.; Beck, L. *Macromolecules* **1977**, *10*, 213.
(24) Tanabe, Y. *J. Polym. Sci., Polym. Phys. Ed.* **1985**, *23*, 601.
(25) Khare, R. S.; Paulaitis, M. E., accepted in *Chem. Eng. Sci.*
(26) Reed, T. M.; Gubbins, K. E. *Applied Statistical Mechanics*; Butterworth-Heinemann: Stoneham, MA, 1973.
(27) Claessens, M.; Ferrario, M.; Ryckaert, J.-P. *Mol. Phys.* **1983**, *50*, 217.
(28) Theodorou, D. N., University of California at Berkeley, personal communication, 1992.
(29) Rapold, R.; Suter, U. W., ETH, Zurich, unpublished results.
(30) Burley, S. K.; Petsko, G. A. *J. Am. Chem. Soc.* **1986**, *108*, 7995.
(31) Brooks, B. R.; Bruccoleri, R. E.; Olafson, B. D.; States, D. J.; Swaminathan, S.; Karplus, M. *J. Comput. Chem.* **1983**, *4*, 187.
(32) Yoon, D. Y.; Sundararajan, P. R.; Flory, P. J. *Macromolecules* **1975**, *8*, 776.
(33) Brandrup, J.; Immergut, E. H. *Polymer Handbook*; John Wiley and Sons: New York, 1989.
(34) Lazaridis, T.; Paulaitis, M. E., submitted for publication in *J. Am. Chem. Soc.*
(35) Bovey, F. A.; Hood, F. P., III; Anderson, E. W.; Snyder, L. C. *J. Chem. Phys.* **1965**, *42*, 3900.
(36) Johnson, L. F.; Heatley, F.; Bovey, F. A. *Macromolecules* **1970**, *3*, 175.
(37) Flory, P. J. *Principles of Polymer Chemistry*; Cornell University: Ithaca, NY, 1953.
(38) Weeks, J. D.; Chandler, D.; Andersen, H. C. *J. Chem. Phys.* **1971**, *54*, 5237.
(39) Lowden, L. J.; Chandler, D. *J. Chem. Phys.* **1975**, *61*, 5228.
(40) Flory, P. J.; Sundararajan, P. R.; DeBolt, L. C. *J. Am. Chem. Soc.* **1974**, *96*, 5015.
(41) Krimm, S. *J. Phys. Chem.* **1953**, *57*, 22.
(42) Schubach, H. R.; Nagy E.; Heise B. *Colloid Polym. Sci.* **1981**, *259*, 789.
(43) Wecker, S. M.; Davidson, T.; Cohen, J. B. *J. Mater. Sci.* **1972**, *7*, 1249.
(44) Theodorou, D. N. Ph.D. Thesis, Massachusetts Institute of Technology, 1985.
(45) *International Tables for X-ray Crystallography*; Macgillavry, C. H., Rieck, G. D., Lonsdale, K., Eds; Kynock: Birmingham, England, 1968; Vol. III, pp 201–207.
(46) Mitchell, G. R.; Windle, A. H. *Polymer* **1984**, *25*, 906.
(47) Song, H. H.; Roe, R. J. *Macromolecules* **1987**, *20*, 2723.
(48) Katz, J. R. *Trans. Faraday Soc.* **1936**, *32*, 77.